PROCEEDINGS OF SCIENCE

Direct measurement of cosmic neon, magnesium, and silicon fluxes with DAMPE

Elisabetta Casilli,^{a,b,†,*} **Francesca Alemanno,**^{a,b} **Paolo Bernardini,**^{a,b}
Francesco de Palma,^{a,b} **Essna Ghose,**^{a,b} **Antonio Surdo**^{b} **and**
Chuan Yue^{c} **on behalf of the DAMPE Collaboration**

[a] *Dipartimento di Matematica e Fisica E. De Giorgi, Università del Salento, I-73100 Lecce, Italy*
[b] *Istituto Nazionale di Fisica Nucleare (INFN) - Sezione di Lecce, I-73100, Lecce, Italy*
[c] *Key Laboratory of Dark Matter and Space Astronomy, Purple Mountain Observatory, Chinese Academy of Sciences, Nanjing 210023, China.*

E-mail: `elisabetta.casilli@le.infn.it`, `elisabetta.casilli@gssi.it`

The Dark Matter Particle Explorer (DAMPE) is a satellite-based detector optimized for precise Galactic cosmic ray studies up to hundreds of TeV. Since its launch on December 17th, 2015, DAMPE has been continuously collecting data on high-energy cosmic particles with excellent statistics and particle identification capabilities, thanks to a large geometric factor and a very good energy resolution. In this contribution, the latest advancements concerning the direct measurement of the energy spectra of cosmic-ray neon, magnesium, and silicon nuclei obtained by DAMPE will be presented. Precise knowledge of these spectral measurements could provide valuable insights into the origin, acceleration, and propagation processes of cosmic rays in the Galaxy.

39th International Cosmic Ray Conference (ICRC2025)
15–24 July 2025
Geneva, Switzerland

ICRC 2025
The Astroparticle Physics Conference
Geneva July 15-24, 2025

---

[*] Speaker

[†] Now at Gran Sasso Science Institute (GSSI), Via Iacobucci 2, I-67100 L'Aquila, Italy and Istituto Nazionale di Fisica Nucleare (INFN) - Laboratori Nazionali del Gran Sasso, I-67100 Assergi, L'Aquila, Italy.

© Copyright owned by the author(s) under the terms of the Creative Commons
Attribution-NonCommercial-NoDerivatives 4.0 International License (CC BY-NC-ND 4.0).

1. Introduction

Cosmic rays (CRs) are high-energy particles originating from astrophysical sources both within and beyond our Galaxy. Their study provides crucial insights into the fundamental processes shaping the Universe, including CR acceleration and subsequent propagation through the interstellar medium. In recent years, several experiments have revealed distinct features in the CR spectra, showing unexpected deviations from the single power-law behaviour predicted by shock acceleration mechanisms for protons and heavier nuclei below 3-4 PeV, where the so-called "knee" of the all-particle spectrum occurs [1–3]. The study of the elemental composition and fluxes of individual CR species plays a key role in unravelling the mechanisms governing CR acceleration and propagation within the Galaxy. One of the most intriguing aspects of CR physics is the study of intermediate-mass nuclei, such as neon, magnesium, and silicon. These elements exhibit spectral behaviours different from those of lighter nuclei such as helium, carbon, and oxygen. Such differences may indicate the presence of multiple source classes or distinct propagation effects [4, 5]. A complete understanding of these variations is essential for refining current astrophysical models. At present, the measurements of the intermediate-mass nuclei remain scarce, particularly in those high-energy regions (>1 TeV/nucleon) which cannot be reached by satellite spectrometer-type experiments or balloon-borne detectors, due to limited statistical and instrumental uncertainties [5–7].

2. The DAMPE detector

The Dark Matter Particle Explorer (DAMPE) is a satellite-borne experiment designed to investigate several scientific topics, including the measurement of CR spectra up to ~10 TeV for the electromagnetic component ($\gamma, e^{\pm}$) and up to hundreds of TeV for protons and nuclei, as well as the search for indirect signatures of dark matter. The instrument is composed of four sub-detectors: a plastic scintillator detector (PSD), a silicon-tungsten tracker-converter (STK), a bismuth germanium oxide (BGO) calorimeter, and a neutron detector (NUD). The PSD consists of 82 bars arranged in two orthogonal planes (X and Y views), each composed of two staggered layers (four layers in total). It is designed to distinguish gamma rays from charged particles and to measure their absolute charge. The STK, composed of six planes of silicon strips and three interleaved tungsten layers, measures particle trajectories and facilitates photon conversion into e^+e^- pairs. The BGO calorimeter, with 14 layers of 22 bars each (corresponding to a depth of ~32 radiation lengths and ~1.6 nuclear interaction lengths), measures the particle energy and discriminates between hadronic and electromagnetic showers. Finally, the NUD, made of four boron-loaded plastic scintillators, enhances the separation between electromagnetic and hadronic events.

3. Data sample

This analysis is based on data collected from January 1, 2016 to December 31, 2023, with a live time of 1.92×10^8 s, corresponding to 76% of the total operational time. Periods affected by instrumental dead time, on-orbit calibration, or passages through the South Atlantic Anomaly (SAA) are excluded. The analysis is validated through simulations performed with the GEANT4

PoS(ICRC2025)024

PoS(ICRC2025)024

toolkit [8], using the FTFP_BERT physics list in the range from 100 GeV to 1 PeV, with a smooth transition to EPOS-LHC for particles above 10 TeV/n, implemented within the CRMC framework[1].

4. Event selection criteria

Pre-selection

An initial selection is applied to retain only well-reconstructed and well-contained events. Events initiating showers at the top of the calorimeter are identified by requiring activation of the High Energy Trigger (HET), which occurs when the energy deposition exceeds 10 MIPs[2] in the first three BGO layers and 2 MIPs in the fourth [9]. To avoid effects due to geomagnetic rigidity cut-off and solar particles, events with total calorimetric energy deposition (E_{BGO}) below 100 GeV are excluded. To ensure good shower containment, events are rejected if the maximum energy deposition occurs at the calorimeter edges in the second, third, or fourth BGO layer. Additionally, the maximum energy deposition in a single layer must remain below 35% of E_{BGO} to suppress badly reconstructed horizontal events.

Track selection

Track reconstruction is performed with a dedicated Machine Learning (ML) tool developed for DAMPE, which is described in detail in Ref. [10]. The reconstructed trajectory must be fully contained within both the PSD and BGO fiducial volumes. To reduce background from lighter nuclei (mainly proton and helium), the average signal in the first STK plane must exceed 1200 ADC counts, corresponding to the signal of ~18 MIPs.

Charge selection

Charge reconstruction is performed using PSD signals along the identified track. A dedicated algorithm applies corrections for path length, light attenuation, and light-yield saturation [11]. Events are selected if the charges reconstructed in the X and Y views agree within $|Q_Y - Q_X| < 2$. The final charge estimate is obtained as the path length-weighted average:

$$Q^{\mathrm{PSD}} = \frac{\sum_i Q_i \, L_i}{\sum_i L_i}, \tag{1}$$

where Q_i is the charge measured in the ith PSD layer and L_i is the traversed path length through the crossed bar. This reduces the weight of events crossing the corners of PSD bars, where short path lengths ($\ll 10\,\mathrm{mm}$) lead to large relative fluctuations. Figure 1a shows the Q^{PSD} spectrum at different selection stages, from pre-selection to the PSD consistency cut. This last selection, together with the STK charge requirement, significantly improves the separation of neon, magnesium, and silicon peaks, as well as heavier nuclei. The final charge selection is performed by fitting Q^{PSD} in different bins of E_{BGO} with a *Langaus* function (a convolution of Landau and Gaussian distributions). The Most Probable Values (MPVs) and widths (σ) extracted from the fits define the energy-dependent charge windows, illustrated by dashed lines in Figure 1b as a function of E_{BGO}.

---

[1] Cosmic Ray Monte Carlo Package (CRMC), `https://zenodo.org/records/5270381`

[2] The energy deposition of a Minimum Ionizing Particle (MIP) in the BGO calorimeter corresponds to ~23 MeV.

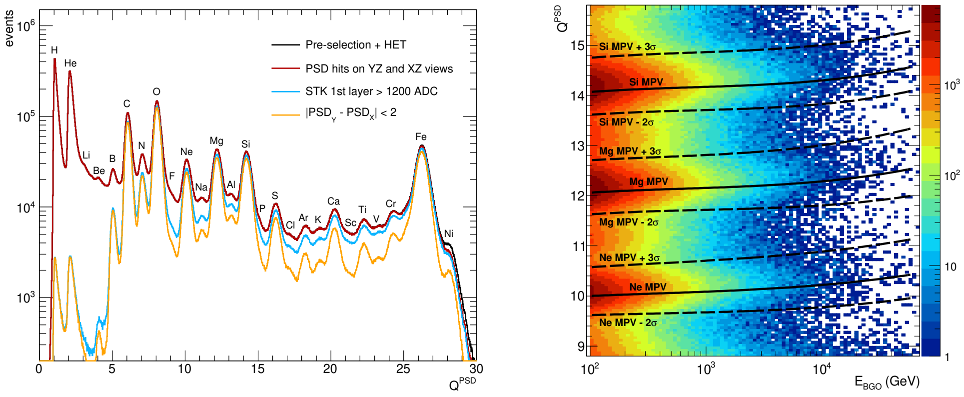

(a) **(b)**

Figure 1: PSD charge spectrum at different selection steps (a) and as a function of E_{BGO} (b). The preliminary charge selection ranges for neon, magnesium, and silicon candidates are indicated by dashed lines.

5. Contamination estimation

Residual contamination from neighbouring nuclei may still affect the selected charge regions. To quantify this, a template-fitting procedure is applied to the Q^{PSD} distributions in several E_{BGO} intervals using the RooFit toolkit[3], with MC-based templates for nuclei from carbon to silicon. Figure 2 shows examples of template fits for neon; similar analyses are performed for magnesium and silicon. The contamination fractions are subtracted from the data before the flux calculation:

$$\tilde{N}_{\mathrm{obs},i} = (1 - f_{\mathrm{tot},i})\, N_{\mathrm{obs},i} \tag{2}$$

where $N_{\mathrm{obs},i}$ is the number of observed events in the ith E_{BGO} bin, $f_{\mathrm{tot},i}$ is the total contamination fraction, and $\tilde{N}_{\mathrm{obs},i}$ is the background-subtracted count. Figure 3 shows the contamination fractions for neon, magnesium, and silicon candidates, with individual contributions from neighbouring nuclei (coloured lines) and the total contamination (black points).

6. Effective acceptance and unfolding procedure

After applying the selection cuts, the effective detector acceptance $A_{\mathrm{eff},i}$ is derived from MC simulations as:

$$A_{\mathrm{eff},i} = A_{\mathrm{gen}} \frac{N_{\mathrm{pass},i}}{N_{\mathrm{gen},i}} \tag{3}$$

where A_{gen} is the geometrical factor for event generation, $N_{\mathrm{gen},i}$ is the number of generated events in the ith energy bin, and $N_{\mathrm{pass},i}$ is the number of events passing all cuts.

Since the calorimeter thickness is limited, the energy deposited by a hadronic CR particle represents only a fraction of its primary energy. To recover the true spectra, a Bayesian unfolding procedure is applied, following the approach of Ref. [12]. The unfolded event distribution in the ith

---

[3] ROOT RooFit toolkit. `https://root.cern/manual/roofit/`.

PoS(ICRC2025)024

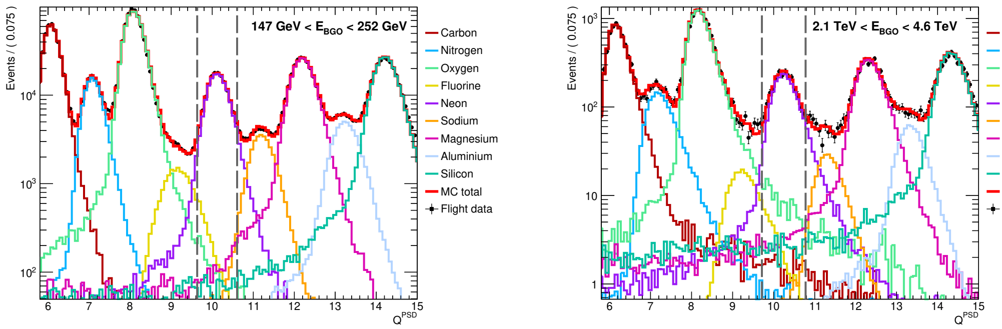

(a) **(b)**

Figure 2: Neon template fits for $147 < E_{\rm BGO} < 252$ GeV (a) and $2.1 < E_{\rm BGO} < 4.6$ TeV (b). Flight data (black points) are compared with MC templates for nuclei from carbon to silicon, as indicated in the legend. The total MC contribution is shown by the red line.

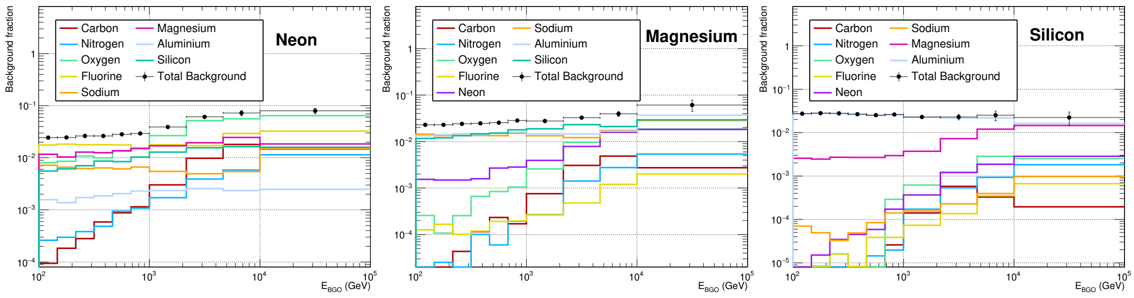

(a) **(b)** **(c)**

Figure 3: Background fractions for neon (a), magnesium (b), and silicon (c), estimated from template fits. Individual contributions are shown according to the coloured legend, while the total background is represented by the black points.

bin of true energy, $N(E_{{\rm true},i})$, is obtained as:

$$N(E_{{\rm true},i}) = \sum_{j=1}^{n} P\left(E_{{\rm true},i} | E_{{\rm obs},j}\right)\; N(E_{{\rm obs},j}), \tag{4}$$

where $N(E_{\rm obs}, j)$ is the number of observed events in the jth deposited-energy bin and $P(E_{\rm true}, i | E_{\rm obs}, j)$ is the unfolding matrix derived from MC simulations. Deposited energies are corrected for BGO saturation [13], while Birk's quenching effects are also taken into account in the simulation [14, 15].

7. Uncertainty estimation

Systematic uncertainties are evaluated from several contributions, including selection efficiencies, background subtraction, and hadronic models in MC simulations:

$$\sigma_{\rm sys} = \sqrt{\sigma^2_{\rm HET} + \sigma^2_{\rm PSD} + \sigma^2_{\rm STK\ charge} + \sigma^2_{\rm STK\ fiducial} + \sigma^2_{\rm bkg}} \tag{5}$$

PoS(ICRC2025)024

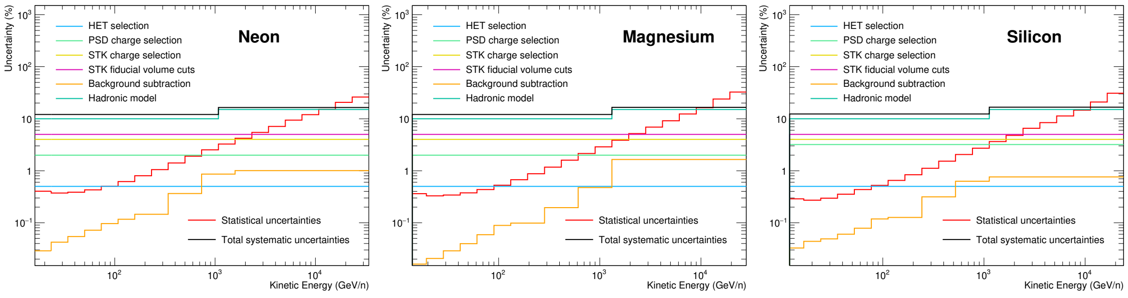

(a) **(b)** **(c)**

Figure 4: Statistical and systematic uncertainties on the energy spectra of neon (a), magnesium (b), and silicon (c) nuclei.

The agreement between data and simulation is within 0.5% for the HET efficiency (σ_{HET}), 2% (neon, magnesium) and 3.2% (silicon) for the PSD charge efficiency (σ_{PSD}), 4% for STK charge efficiency ($\sigma_{\text{STK charge}}$), and 5% for STK containment ($\sigma_{\text{STK fiducial}}$). The uncertainty on background subtraction (σ_{bkg}) reflects the template-fit errors on contamination fractions. Model-dependent uncertainties are usually evaluated through comparison with ion beam-test data or alternative hadronic interaction models, such as FLUKA [16]. Although dedicated studies for neon, magnesium, and silicon are not yet available, comparisons on oxygen provide an estimate of their order of magnitude, used here as a preliminary evaluation. A summary of systematic uncertainties is presented in Figure 4.

8. Preliminary results

The differential flux Φ_i as a function of the kinetic energy is computed as follows:

$$\Phi_i = \frac{\Delta N_i}{\Delta T \, A_{\text{eff},i} \, \Delta E_i} \tag{6}$$

where N_i is the number of unfolded events, ΔT the live time, $A_{\text{eff},i}$ the effective acceptance, and ΔE_i the bin width. The fluxes are converted to kinetic energy per nucleon, assuming pure compositions of ^{20}Ne, ^{24}Mg, and ^{28}Si. Figure 5 shows the resulting spectra compared with previous measurements [6, 7, 17–20].

This work presents the preliminary DAMPE results on the measurement of the CR energy spectra of neon, magnesium, and silicon, covering the range from a few hundred GeV up to ~100 TeV, and providing new high-precision data in the intermediate-mass nuclei region. The DAMPE measurements confirm the presence of a spectral hardening in these nuclei, as previously indicated by other experiments [5, 7]. Ongoing studies aim to refine the evaluation of systematic uncertainties, including those related to hadronic interaction models, selection efficiencies, and the isotopic composition assumption, and to extend the measurement to higher energies. In the near future, DAMPE will provide improved spectra of CR neon, magnesium, and silicon with extended coverage at the highest energies.

PoS(ICRC2025)024

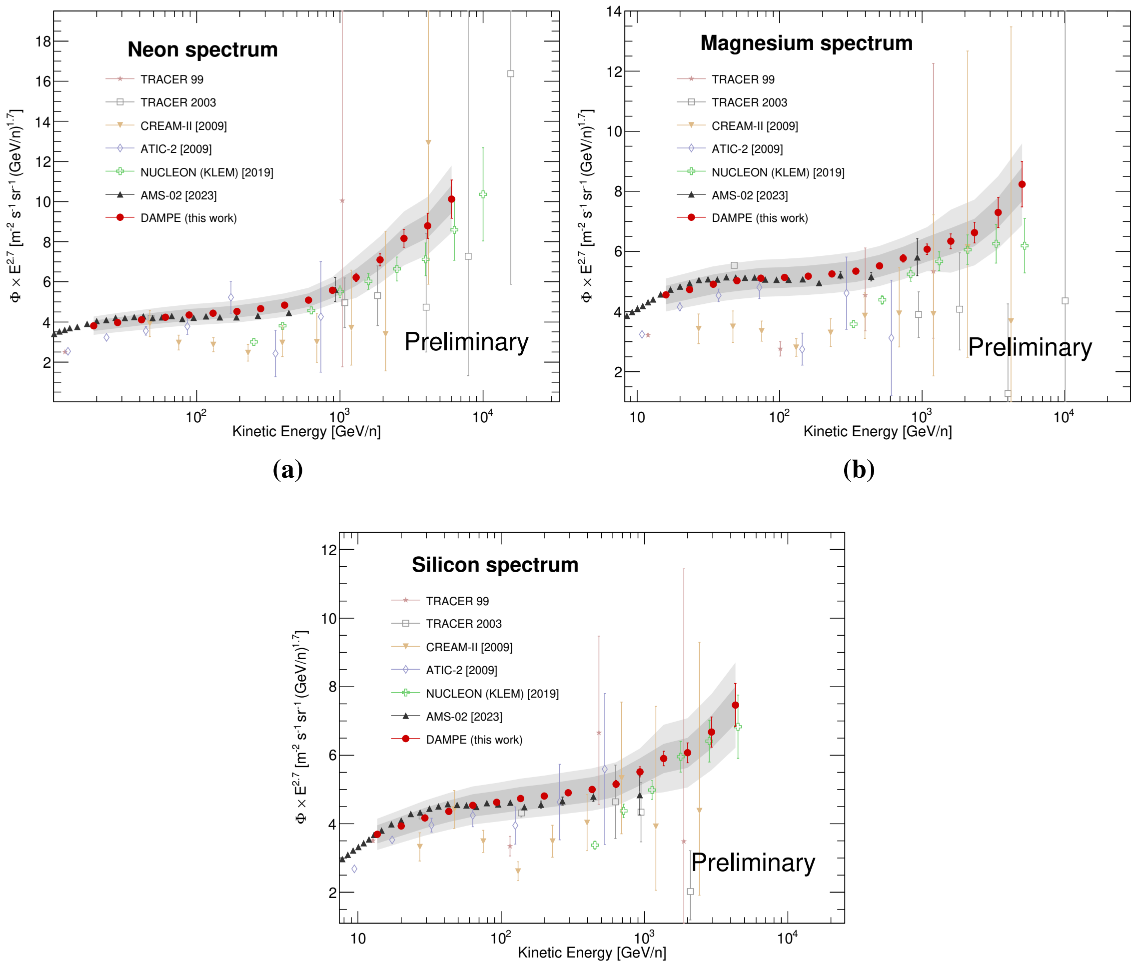

(a) **(b)**

(c)

Figure 5: DAMPE spectra of neon (a), magnesium (b), and silicon (c) as a function of kinetic energy per nucleon, multiplied by $E^{2.7}$ and compared with results from TRACER [17, 18], CREAM-II [6], ATIC-2 [19], NUCLEON-KLEM [7], and AMS-02 [20]. Error bars indicate statistical uncertainties. The inner band shows the systematic uncertainty from the analysis, while the outer band includes the overall systematic uncertainty, accounting also for the hadronic contribution.

Acknowledgements

The DAMPE mission was funded by the strategic priority science and technology projects in space science of Chinese Academy of Sciences. In China the data analysis is supported by the National Key Research and Development Program of China (No. 2022YFF0503302), the National Natural Science Foundation of China (No. 12220101003, No. 12275266, No. 12003076, No. 12022503, and No. 12103094), the Strategic Priority Program on Space Science of Chinese Academy of Sciences (No. E02212A02S), the Youth Innovation Promotion Association of CAS and the New Cornerstone Science Foundation through the XPLORER PRIZE. In Europe the activities and data analysis are supported by the Swiss National Science Foundation (SNSF), Switzerland,

PoS(ICRC2025)024

the National Institute for Nuclear Physics (INFN), Italy, and the European Research Council (ERC) under the European Union's Horizon 2020 research and innovation program (No. 851103).

References

[1] Q. An *et al.* (DAMPE Collaboration), Sci. Adv. 5 (2019) eaax3793.

[2] F. Alemanno *et al.* (DAMPE Collaboration), Phys. Rev. Lett. 126 (2021) 201102.

[3] F. Alemanno *et al.* (DAMPE Collaboration), Phys. Rev. D 109 (2024) L121101.

[4] B. Schroer, C. Evoli and P. Blasi, Phys. Rev. D 103 (2021) 123010.

[5] M. Aguilar *et al.* (AMS Collaboration), Phys. Rev. Lett. 124 (2020) 211102.

[6] H. S. Ahn *et al.*, Astrophys. J. 707 (2009) 593.

[7] V. Grebenyuk *et al.* Adv. Space Res. 64 (2019) 2546.

[8] S. Agostinelli *et al.*, Nucl. Instrum. Methods Phys. Res. A, 506 (2003) 250.

[9] Y.-Q. Zhang *et al.* Res. Astron. Astrophys. 19 (2019) 123.

[10] A. Tykhonov *et al.*, Astropart. Phys. 146 (2023) 102795.

[11] T. Dong *et al.*, Astropart. Phys. 105 (2019) 31.

[12] G. D'Agostini, Nucl. Instrum. Meth. A 362 (1995) 487.

[13] C. Yue *et al.*, Nucl. Instrum. Meth. A 984 (2020) 164645.

[14] J. B. Birks, Proc. Phys. Soc. A 64 (1951), 874.

[15] Z. Cheng *et al.* Nucl. Instrum. Meth. A 1055 (2023) 168470.

[16] A. Ferrari *et al.*, CERN Yellow report 10 (2005).

[17] F. Gahbauer *et al.* Astrophys. J. 607 (2004) 333.

[18] M. Ave *et al.* Astrophys. J. 678 (2008) 262.

[19] A. D. Panov *et al.* Bull. Russ. Acad. Sci.: Phys. 73 (2009) 564.

[20] M. Aguilar *et al.* (AMS Collaboration), Phys. Rev. Lett. 130 (2023) 211002.

PoS(ICRC2025)024

PoS(ICRC2025)024

DAMPE Collaboration

Francesca Alemanno[1,2], Qi An[3,4], Philipp Azzarello[5], Felicia Carla Tiziana Barbato[6,7], Paolo Bernardini[1,2], Xiao-Jun Bi[8,9], Hugo Valentin Boutin[5], Irene Cagnoli[6,7], Ming-Sheng Cai[10,11], Elisabetta Casilli[1,2][*], Jin Chang[10,11], Deng-Yi Chen[10], Jun-Ling Chen[12], Zhan-Fang Chen[12], Zi-Xuan Chen[12,8], Paul Coppin[5], Ming-Yang Cui[10], Tian-Shu Cui[13], Ivan De Mitri[6,7], Francesco de Palma[1,2], Adriano Di Giovanni[6,7], Tie-Kuang Dong[10], Zhen-Xing Dong[13], Giacinto Donvito[14], Jing-Lai Duan[12], Kai-Kai Duan[10], Rui-Rui Fan[9], Yi-Zhong Fan[10,11], Fang Fang[12], Kun Fang[9], Chang-Qing Feng[3,4], Lei Feng[10], Sara Fogliacco[6,7], Jennifer Maria Frieden[5][†], Piergiorgio Fusco[14,15], Min Gao[9], Fabio Gargano[14], Essna Ghose[1,2], Ke Gong[9], Yi-Zhong Gong[10], Dong-Ya Guo[9], Jian-Hua Guo[10,11], Shuang-Xue Han[13], Yi-Ming Hu[10], Guang-Shun Huang[3,4], Xiao-Yuan Huang[10,11], Yong-Yi Huang[10], Maria Ionica[16], Lu-Yao Jiang[10], Wei Jiang[10], Yao-Zu Jiang[16][‡], Jie Kong[12], Andrii Kotenko[5], Dimitrios Kyratzis[6,7], Shi-Jun Lei[10], Bo Li[10,11], Manbing Li[5], Wei-Liang Li[13], Wen-Hao Li[10], Xiang Li[10,11], Xian-Qiang Li[13], Yao-Ming Liang[13], Cheng-Ming Liu[16], Hao Liu[10], Jie Liu[12], Shu-Bin Liu[3,4], Yang Liu[10], Francesco Loparco[14,15], Miao Ma[13], Peng-Xiong Ma[10], Tao Ma[10], Xiao-Yong Ma[13], Giovanni Marsella[1,2][§], Mario-Nicola Mazziotta[14], Dan Mo[12], Yu Nie[3,4], Xiao-Yang Niu[12], Andrea Parenti[6,7][¶], Wen-Xi Peng[9], Xiao-Yan Peng[10], Chiara Perrina[5][‖], Enzo Putti-Garcia[5], Rui Qiao[9], Jia-Ning Rao[13], Yi Rong[3,4], Andrea Serpolla[5], Ritabrata Sarkar[6,7], Pierpaolo Savina[6,7], Zhi Shangguan[13], Wei-Hua Shen[13], Zhao-Qiang Shen[10], Zhong-Tao Shen[3,4], Leandro Silveri[6,7][**], Jing-Xing Song[13], Hong Su[12], Meng Su[17], Hao-Ran Sun[3,4], Zhi-Yu Sun[12], Antonio Surdo[2], Xue-Jian Teng[13], Andrii Tykhonov[5], Gui-Fu Wang[3,4], Jin-Zhou Wang[9], Lian-Guo Wang[13], Shen Wang[10], Xiao-Lian Wang[3,4], Yan-Fang Wang[3,4], Da-Ming Wei[10,11], Jia-Ju Wei[10], Yi-Feng Wei[3,4], Di Wu[9], Jian Wu[10,11], Sha-Sha Wu[13], Xin Wu[5], Zi-Qing Xia[10], Zheng Xiong[6,7], En-Heng Xu[3,4], Hai-Tao Xu[13], Jing Xu[10], Zhi-Hui Xu[12], Zi-Zong Xu[3,4], Zun-Lei Xu[10], Guo-Feng Xue[13], Ming-Yu Yan[3,4], Hai-Bo Yang[12], Peng Yang[12], Ya-Qing Yang[12], Hui-Jun Yao[12], Yu-Hong Yu[12], Qiang Yuan[10,11], Chuan Yue[10], Jing-Jing Zang[10][††], Sheng-Xia Zhang[12], Wen-Zhang Zhang[13], Yan Zhang[10], Ya-Peng Zhang[12], Yi Zhang[10,11], Yong-Jie Zhang[12], Yong-Qiang Zhang[10], Yun-Long Zhang[3,4], Zhe Zhang[10], Zhi-Yong Zhang[3,4], Cong Zhao[3,4], Hong-Yun Zhao[12], Xun-Feng Zhao[13], Chang-Yi Zhou[13], Xun Zhu[10][‡‡], and Yan Zhu[13]

[1]Dipartimento di Matematica e Fisica E. De Giorgi, Università del Salento, I-73100, Lecce, Italy
[2]Istituto Nazionale di Fisica Nucleare (INFN) - Sezione di Lecce, I-73100, Lecce, Italy
[3]State Key Laboratory of Particle Detection and Electronics, University of Science and Technology of China, Hefei 230026, China
[4]Department of Modern Physics, University of Science and Technology of China, Hefei 230026, China
[5]Department of Nuclear and Particle Physics, University of Geneva, CH-1211, Switzerland
[6]Gran Sasso Science Institute (GSSI), Via Iacobucci 2, I-67100 L'Aquila, Italy
[7]Istituto Nazionale di Fisica Nucleare (INFN) - Laboratori Nazionali del Gran Sasso, I-67100 Assergi, L'Aquila, Italy
[8]University of Chinese Academy of Sciences, Beijing 100049, China
[9]Particle Astrophysics Division, Institute of High Energy Physics, Chinese Academy of Sciences, Beijing 100049, China
[10]Key Laboratory of Dark Matter and Space Astronomy, Purple Mountain Observatory, Chinese Academy of Sciences, Nanjing 210023, China
[11]School of Astronomy and Space Science, University of Science and Technology of China, Hefei 230026, China
[12]Institute of Modern Physics, Chinese Academy of Sciences, Lanzhou 730000, China
[13]National Space Science Center, Chinese Academy of Sciences, Nanertiao 1, Zhongguancun, Haidian district, Beijing 100190, China
[14]Istituto Nazionale di Fisica Nucleare, Sezione di Bari, via Orabona 4, I-70126 Bari, Italy
[15]Dipartimento di Fisica "M. Merlin", dell'Università e del Politecnico di Bari, via Amendola 173, I-70126 Bari, Italy
[16]Istituto Nazionale di Fisica Nucleare (INFN) - Sezione di Perugia, I-06123 Perugia, Italy
[17]Department of Physics and Laboratory for Space Research, the University of Hong Kong, Hong Kong SAR, China

---

[*] Now at Gran Sasso Science Institute (GSSI), Via Iacobucci 2, I-67100 L'Aquila, Italy.

[†] Now at Institute of Physics, Ecole Polytechnique Fédérale de Lausanne (EPFL), CH-1015 Lausanne, Switzerland.

[‡] Also at Dipartimento di Fisica e Geologia, Università degli Studi di Perugia, I-06123 Perugia, Italy.

[§] Now at Dipartimento di Fisica e Chimica "E. Segrè", Università degli Studi di Palermo, via delle Scienze ed. 17, I-90128 Palermo, Italy.

[¶] Now at Inter-university Institute for High Energies, Universitè Libre de Bruxelles, B-1050 Brussels, Belgium.

[‖] Now at Institute of Physics, Ecole Polytechnique Fédérale de Lausanne (EPFL), CH-1015 Lausanne, Switzerland.

[**] Now at New York University Abu Dhabi, Saadiyat Island, Abu Dhabi 129188, United Arab Emirates.

[††] Also at School of Physics and Electronic Engineering, Linyi University, Linyi 276000, China.

[‡‡] Also at School of computing, Nanjing University of Posts and Telecommunications, Nanjing 210023, China.